Environmental Science & Technology

Article

Cite This: Environ. Sci. Technol. 2018, 52, 5875−5883

pubs.acs.org/est

Understanding Electrochemically Activated Persulfate and Its Application to Ciprofloxacin Abatement

Laura W. Matzek,[†] Matthew J. Tipton,[†] Abigail T. Farmer,[‡] Andrew D. Steen,[§] and Kimberly E. Carter*[,†]

[†]Department of Civil and Environmental Engineering, University of Tennessee, 325 John D. Tickle Building, Knoxville, Tennessee 37996-2313, United States

[‡]Department of Chemistry, University of Tennessee, 552 Buehler Hall, Knoxville, Tennessee 37996-1600, United States

[§]Department of Earth and Planetary Sciences, University of Tennessee, 602 Strong Hall, Knoxville, Tennessee 37996-1526, United States

Supporting Information

ABSTRACT: This study offers insight into the roles anodic and cathodic processes play in electrochemically activated persulfate (EAP) and screens EAP as a viable technique for ciprofloxacin degradation in wastewater. Sulfate radical formation at a boron-doped diamond (BDD) anode and persulfate activation at a graphite cathode were experimentally elucidated using different electrolytes and electrochemical setups. Rapid ciprofloxacin transformation occurred via pseudo-first-order mechanisms with respect to ciprofloxacin in persulfate electrolyte, reaching 84% removal in 120 min using EAP. Transformation pathways were compared to those in nitrate and sulfate electrolytes. Ciprofloxacin removal rates in the electrochemical system were 88% and 33% faster in persulfate than nitrate and sulfate electrolytes, respectively. Total organic carbon removal rates were 93% and 48% faster in persulfate than nitrate and sulfate, respectively. Use of sulfate electrolyte resulted in removal rates 6−7 times faster than those in nitrate solution. Accelerated removal in sulfate was attributed to anodic sulfate radical formation, while enhanced removal in persulfate was associated with cathodic persulfate activation and nonradical persulfate activation at the BDD anode. Quenching experiments indicated both sulfate radicals and hydroxyl radicals contributed to degradation. Comparisons between platinum and graphite cathodes showed similar cathodic persulfate activation and ciprofloxacin degradation.

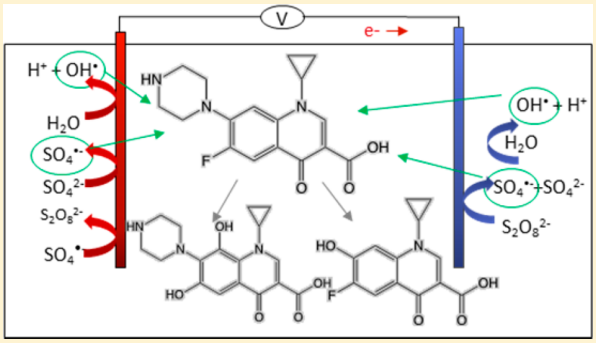

INTRODUCTION

Ciprofloxacin, a fluoroquinolone antibiotic, is regarded as a high-risk environmental contaminant that enters aquatic ecosystems through incomplete breakdown by traditional wastewater treatment plants (WWTP).[1−6] Hospital effluent is a primary source of ciprofloxacin entering WWTPs.[2,4,7] Other sources of environmental ciprofloxacin include pharmaceutical manufacturer effluent and agricultural runoff, which are often untreated.[6,8]

Point source treatment of contaminated wastewaters is a proposed mitigation strategy. Electrochemical advanced oxidation processes (EAOPs) are a candidate for removal of fluoroquinolone antibiotics, pharmaceuticals and other targeted pollutants like X-ray contrast media.[9−14] EAOPs offer the advantage of eliminating total organic carbon (TOC), which may contain harmful transformation byproducts.[15,16]

The EAOP mechanism is attributed to hydroxyl radical formation ($E°$ = 2.74 V) that can occur at anode surfaces such as BDD, tin dioxide, and lead dioxide (eq 1).[13,14,16−18] These hydroxyl radicals react to degrade organic contaminants and propagate other radicals, which can participate in degradation reactions.[13,14,16−18] Additionally, oxidation of the target contaminant by direct electron transfer at the anode can occur.[18,19]

$$H_2O \rightarrow OH\cdot + H^+ + e^- \quad (1)$$

Recent studies examined the role of sulfate radicals ($E°$ = 2.5−3.1 V) in EAOP.[11,20] Sulfate radicals form anodically using BDD electrodes (eq 2), and will degrade many organic analytes.[11,21] These radicals can also form reactive hydroxyl radicals (eq 3).[21] Higher removal rates for diatrizoate and carbamazepine were achieved in sulfate versus nitrate electrolyte, which was credited to anodic sulfate radical formation.[11,20]

$$SO_4^{2-} \rightarrow SO_4^{\bullet -} + e^- \quad (2)$$

$$SO_4^{\bullet -} + H_2O \rightarrow SO_4^{2-} + OH\cdot + H^+ \quad (3)$$

Received: January 2, 2018
Revised: April 12, 2018
Accepted: April 13, 2018
Published: April 13, 2018

DOI: 10.1021/acs.est.8b00015
Environ. Sci. Technol. 2018, 52, 5875−5883

Electrochemically activated persulfate (EAP) analyte removal has not been widely addressed except in cases where iron is a coactivator.[21,22] Studies investigating EAP without iron suggest persulfate activation, through direct electron transfer at the cathode, creates sulfate radicals (eq 4).[23,24]

$$S_2O_8^{2-} + e^- \rightarrow SO_4^{2-} + SO_4^{\bullet -} \quad (4)$$

Recent studies found persulfate addition to electrochemical abatement of industrial wastewater improved removal of dinitrotoluene and aniline, but did not compare the effects created by sulfate addition.[23,24] Another report indicated that persulfate addition to sodium chloride electrolyte increased removal of malachite green and 2,4-dinitrophenol while sulfate did not, though differences between these electrolytes was not the focus.[25] Farhat et al. (2015) found that persulfate addition to nitrate electrolyte did not result in as fast of a diatrizoate removal rate as in pure sulfate.[11] However, equimolar amounts of persulfate and sulfate were not compared and cathodic persulfate activation was not explored.[11]

The purpose of this study is to characterize enhanced electrochemical removal of organic species observed in sulfate and persulfate electrolytes, including the roles played by sulfate radical formation at the anode and persulfate activation at the cathode.[24,25] Elucidating the sources and roles reactive species play in sulfate radical-based systems lends insight into appropriate application and design of electrochemical abatement systems. Finally, although fluoroquinolone removal has previously been demonstrated at a BDD anode in synthetic urine and a SnO_2/Sb−Ti anode in sodium sulfate, it has not been evaluated in the EAP system.[13,26] Thus, this study aims to assess EAP's ability to remove ciprofloxacin and investigate removal mechanisms as a step in screening EAP as an appropriate point source treatment for wastewaters with high antibiotic content.[9,13]

MATERIALS AND METHODS

Chemicals. Ciprofloxacin (98%), sodium persulfate (98%), potassium sulfate, sodium nitrate, potassium iodide (99+%), sodium bicarbonate (Acros Organic, Fair Lawn, NJ), optima formic acid, sodium hydroxide, hydrochloric acid, optima methanol (MeOH), *tert*-butanol (TBA), dimethyl sulfoxide (DMSO), and fluoride standard were purchased from Fisher Scientific (Pittsburgh, PA) and 1 N sulfuric acid was from J.T. Baker. Deionized water (DI) (18.2 MΩ-cm) was produced by a Millipore Milli-Q system.

Experimental Setup. Rotating disk electrode (RDE) experiments were performed using a SP-150 potentiostat (Bio-Logic Science Instruments, Knoxville, TN) with a mercury−mercury sulfate reference electrode in single-cell or split-cell configuration, illustrated by Schematic S1a,b (Supporting Information). A multispeed rotator (Pine Research Instrumentation, PRI, Durham, NC) was set to 2000 rpm for RDE experiments with bulk mixing with a magnetic stir-bar. Anodes (0.5 cm O.D., 0.196 cm^2 surface area) were a change-disk RDE tip (PRI) with BDD electrode insert (Fraunhofer Center for Coatings and Diamond Technologies, East Lansing, MI), or fixed-disk platinum (Pt) RDE tip (PRI). The potential window for the BDD was −1.2 to +2.5 V vs SHE. Cathodes were Electron Microscopy Science graphite (Gr) rods (0.30 cm O.D) (Fisher Scientific, Pittsburgh, PA), or a platinum wire (0.5 mm O.D.) (PRI). Cathodic surface areas exposed to solution were 4.8 cm^2 for graphite and 3.69−4.76 cm^2 for Pt. Potential windows for cathode materials are −1.5 to +1.5 V (Gr) and −0.85 to +1.9 V (Pt).[27]

For single-cell persulfate experiments, 200 mL of 22 mmol L^{-1} persulfate was electrolyzed and sampled periodically. Single-cell ciprofloxacin experiments used 50 mL of 0.171 mmol L^{-1} ciprofloxacin (in 0.003% sulfuric acid to aid dissolution) mixed with 140 mL DI water to a concentration of 0.045 mmol L^{-1} ciprofloxacin. Solution was spiked with 10 mL concentrated electrolyte just before applying constant anodic current density of 76 mA cm^{-2}, unless noted otherwise. Initial concentrations were 0.043 mmol L^{-1} ciprofloxacin plus 22 mmol L^{-1} sulfate or persulfate, or 66 mmol L^{-1} nitrate, maintaining the same ionic strength for all solutions. Quenching experiments were performed by replacing some water with TBA or DMSO to achieve quencher concentration of 2200 mmol L^{-1}, which provided 100:1 quencher to persulfate ratio.[28,29]

Split-cell experiments were performed using 300 mL anodic and 80 mL cathodic compartments. A cation-exchange Chemours 115 Nafion membrane (Fuel Cell Store, College Station, TX), separated the compartments and was experimentally confirmed not to transmit nitrate/sulfate/persulfate anions. Current density of 28.5 mA cm^{-2} was employed due to system physical limitations. For ciprofloxacin removal, outcomes are indicative of behavior in the single-cell reactor, but numerical results are not directly comparable due to current densities utilized.

Experiments were performed in duplicate at 20 °C. Initial pHs averaged 4.5 upon mixing ciprofloxacin and electrolytes for single-cell and split-cell experiments. Average final pHs in the single-cell were 2.5, 6.5, and 8.0 in persulfate, sulfate, and nitrate, respectively. In the split-cell, anode/cathode final pHs were: 7.0/12.0 (nitrate), 4.5/9.0 (sulfate), and 3.0/3.0 (persulfate). pH was not controlled in any experiments as buffer anions can significantly alter the system chemistry confounding interpretation of the results.[18,30−34] As the pH range impacts the kinetics of electrochemical degradation reactions by influencing the active radical species involved (hydroxyl or sulfate),[21] this study aims to understand the natural progression of these reactions, including the possibility that different reaction kinetics may occur due to pH shifts from different species formed in the three electrolytes.

Analytical Methods. Persulfate was analyzed using a ThermoScientific Evolution 600 UV/vis spectrometer (ThermoFisher, Pittsburgh, PA) at 352 nm, respectively, with methodology previously described.[22,35,36]

Waters Sep-Pak tC2 cartridges were used to extract ciprofloxacin for HPLC-UV and HPLC-MS analysis. Cartridges were conditioned with 1 mL of methanol then 1 mL of DI water. A 0.5 mL sample was loaded then extracted using 2 × 1 mL quantities of methanol/0.1% formic acid.[22] The extraction efficiency was 80%, measured by comparing extracted standards to standards made in methanol/0.1% formic acid.

Extracted ciprofloxacin was quantified by separation using a Shimadzu HPLC equipped with binary pumps, a Hypersil Gold column (100 mm × 4.6 mm I.D., 5 μm diameter) (Thermoscientific, Waltham, MA) and a SPD-M20A diode array detector. A gradient eluent separation was used with eluent "A" DI water/0.1% formic acid and eluent "B" acetonitrile/0.1% formic acid. A multistep gradient program varied from 5% to 95% eluent A over 20 min (Table S1). Column temperature was held at 40 °C. Sample absorbance was measured at 278 nm, which was confirmed to be the

DOI: 10.1021/acs.est.8b00015
Environ. Sci. Technol. 2018, 52, 5875−5883

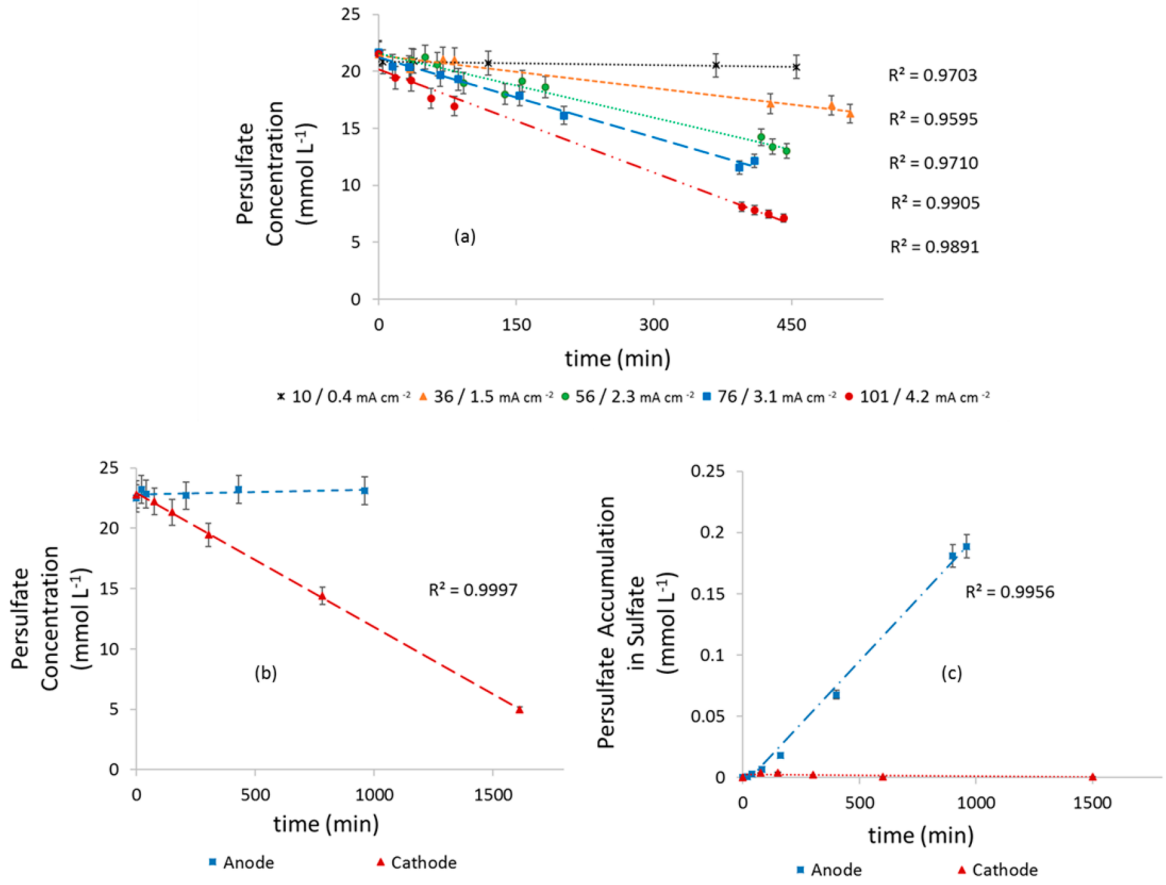

Figure 1. (a) Zero-order persulfate removal over time in a single-cell reactor with $[Persulfate]_0$= 22 mmol L^{-1}. Legend values denote anodic/cathodic current densities. (b) Persulfate concentration versus time with $[Persulfate]_0$= 22 mmol L^{-1} in a split cell reactor. Anodic current density = 28.5 mA cm^{-2} and cathodic current density = 1.2 mA cm^{-2}. (c) Persulfate concentration versus time with $[Sulfate]_0$ = 22 mmol L^{-1} in a split cell reactor. Anodic current density = 28.5 mA cm^{-2} and cathodic current density = 1.2 mA cm^{-2}. (a-c) BDD/Gr anode/cathode pairs. No organic analyte. Error bars represent the 95% confidence interval.

absorbance maximum of ciprofloxacin standards. The instrument detection limit was 0.30 μmol L^{-1} and method detection limit was 0.38 μmol L^{-1}.

Extracts were analyzed for byproducts using ThermoScientific Exactive Plus Orbitrap LC-MS (ThermoFisher, Pittsburgh, PA). A full description of the LC-MS method can be found in the Supporting Information under Method S1, along with Figure S14a−u, which show the mass spectra for different byproducts detected during the analysis of ciprofloxacin degradation.

TOC was analyzed using a Shimadzu TOC-L analyzer with an ASI-L autosampler. Samples were diluted 1:4 with acidified DI water (pH 3.0 with HCl). Statistical parameters for the method were described in a previous study.[22]

Hydrogen peroxide concentrations determined by reacting equal volumes of sample with ammonium metavanadate. Metavanadate solution was prepared with 1 part ammonium metavanadate in 9.5 parts 1 N sulfuric acid at 50 °C, then diluted with DI water to a final concentration of 12 and 114 mM, respectively. Absorbance was measured using the Evolution 600 UV−vis (wavelength 450 nm).[11,37] Absorbance was compared to solutions of known hydrogen peroxide concentrations. Ion chromatography used to analyze fluoride (F^-) concentrations using a Dionex 2100/1100 dual column system with background suppression. pH of all samples was raised to 6, dissociating any potential hydrofluoric acid. Fluoride detection limit was less than 5.2 μmol L^{-1} F^- ions.

RESULTS AND DISCUSSION

Electrochemical Persulfate Decomposition and Regeneration. Persulfate behavior was investigated without an analyte using a single-cell RDE system for three anode/cathode combinations: Pt/Gr, BDD/Gr, and BDD/Pt. The persulfate removal rate was measured to demonstrate the maximum potential persulfate activation rate based on eq 4. For persulfate formation at the anode, this removal rate becomes the net rate of persulfate reduction (or activation) at the cathode and persulfate generation at the anode (eq 5). Similar results were obtained for all electrode combinations with R^2 > 0.95 linear relationship of persulfate decomposition with time. Plots for BDD/Gr (Figure 1a) illustrate these findings. The zero-order mechanism indicates a surface-dominated reaction with the net persulfate reaction rate a function of current density (Figure 2a,b). Persulfate reaction rates were independent of anode material, but were higher using a Gr-cathode compared to a Pt-cathode, as shown in Figure 2a,b. Additional experiments investigating the effects of cathode material for ciprofloxacin

DOI: 10.1021/acs.est.8b00015
Environ. Sci. Technol. 2018, 52, 5875−5883

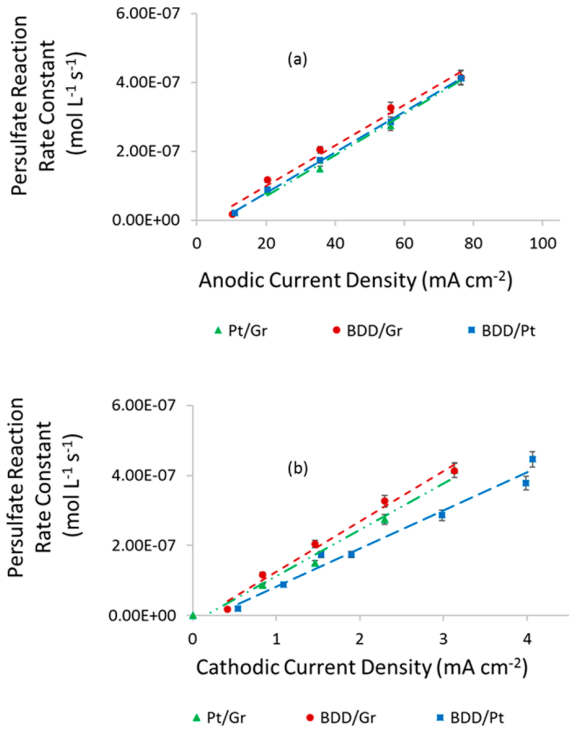

Figure 2. (a) Persulfate zero-order reaction rate constant as a function of anodic current density. (b) Persulfate zero-order reaction rate constant as a function of cathodic current density. Error bars represent the 95% confidence interval.

removal using EAP are described in the Ciprofloxacin Degradation section.

To further explore the role of sulfate radicals in EAOP, electrochemical persulfate removal and generation were examined using split-cell RDE experiments with a BDD/Gr anode/cathode combination. Anodic persulfate generation from sulfate, shown to be a zero-order mechanism in Figure 1c, was used to demonstrate the presence of sulfate radicals, as sulfate-radical based reactions (eq 5) have been shown to be the dominant mechanism of persulfate production at BDD anodes.[38]

$$SO_4^{\bullet -} + SO_4^{-} \rightarrow S_2O_8^{2-} \quad (5)$$

During this process, persulfate becomes available in sulfate solution to initiate nonradical degradation or degradation through persulfate activation at the cathode.[11,24,38] As expected, no persulfate was formed in the sulfate solution from cathodic reactions (Figure 1c) and no hydrogen peroxide was detected in any of the solutions. Further evaluation of H_2O_2 suggests that reaction potentials used were outside the ideal range for H_2O_2 formation.[39] As the solution was not oxygenated, which aids H_2O_2 production (eq S2), this species was determined to have no significant influence in the current EAP system.[39]

Figure 1b shows the persulfate concentration remained constant at the anode, thus persulfate activation by anodically generated hydroxyl radicals was ruled out. Persulfate decomposition at the cathode followed a zero-order mechanism. The zero-order persulfate reaction rate constant of 1.85×10^{-7} mol L^{-1} s^{-1} at a cathodic current density of 1.2 mA cm^{-2} corresponds to the potential sulfate radical formation rate. When the anodic persulfate formation rate of 3.40×10^{-9} mol L^{-1} s^{-1} was subtracted from the cathodic persulfate decomposition rate, the net reaction rate change in the divided cell was 1.82×10^{-7} mol L^{-1} s^{-1}, higher than the 1.5×10^{-7} mol L^{-1} s^{-1} predicted by the single-cell curve in Figure 2a,b at the same current densities (28.5/1.2 mA cm^{-2} anode/cathode, respectively). Differences in single-cell and split-cell reaction rate constants imply the persulfate activation and generation processes may be dependent on one another and are influenced by reactions occurring at the opposite electrode. Experiments determining whether cathodic persulfate decomposition corresponds to sulfate radical formation at the cathode are discussed in the Cyclic Voltammetry and Using Ciprofloxacin To Evaluate Persulfate Activation sections.

Ciprofloxacin Degradation. Removal of ciprofloxacin and TOC was compared for BDD/Pt and BDD/Gr electrode pairs in a single-cell RDE system to establish how cathode materials affect EAP during analyte removal. The pseudo-first-order rate constants (and relevant statistics) with respect to ciprofloxacin for removal by cathode type are shown in Table S2. Ciprofloxacin and TOC degradation rates were statistically insignificant with Pt- and Gr-cathodes. It was concluded that graphite is a suitable substitute for platinum for ciprofloxacin and TOC removal using EAP.

Electrolyte effects on ciprofloxacin removal were compared using the single-cell RDE with nitrate, sulfate or persulfate. Ciprofloxacin degraded rapidly upon electrolysis in persulfate (Figure 3a), reaching 84% of the initial concentration after 120 min and plateauing at 90% after 240 min. The removal rate in sulfate was slower, although similar degrees of removal were achieved within 240 min (Figure 3a). Much slower removal was observed in nitrate, reaching 90% in 24 h (Figure 3b). The ciprofloxacin decay mechanism was pseudo-first-order with respect to ciprofloxacin, as shown in Figures 3a,b and Figure S1. The pseudo-first-order rate constants (and relevant statistics) with respect to ciprofloxacin are shown in Table 1. A 6-fold increase in the overall reaction rate constant was observed using sulfate in place of nitrate electrolyte. This is similar to Radjenovic et al. (2016) findings where using sulfate instead of nitrate electrolyte resulted in a 7-fold increase in reaction rates for iopromide and diatrizoate removal.[20] The current findings, in conjunction with the previously described persulfate experiments, confirm that sulfate does not act as an inert electrolyte when using BDD anodes, rather it participates in degradation reactions, likely through sulfate radical formation. A significant increase of 33% was achieved for the reaction rate constant using persulfate instead of sulfate electrolyte, which may be attributed to cathodic persulfate activation, as described in Cyclic Voltammetry and Using Ciprofloxacin to Evaluate Persulfate Activation sections.

TOC removal followed pseudo-first-order kinetics with respect to total TOC, in sulfate and persulfate (Figure 3c, Table 1). Degradation was less than ciprofloxacin removal. Although the pseudo-first-order fit for nitrate was poor, this model aided quantitative comparison. Nitrate initially produced more rapid TOC degradation than sulfate or persulfate electrolytes, and similar removal was observed for sulfate and persulfate during this initial time frame (Figure S2). However, TOC removal in nitrate quickly plateaued and little removal was observed after the 2 h mark, while persulfate began to show better removal than sulfate. The effect of sulfate over nitrate produced a 7-fold increase in TOC removal rate ($p < 0.0001$). For the time series, the additional TOC removal rate for persulfate versus sulfate was 48%, slightly larger than that observed for the ciprofloxacin relationship (Table 1).

DOI: 10.1021/acs.est.8b00015
Environ. Sci. Technol. 2018, 52, 5875−5883

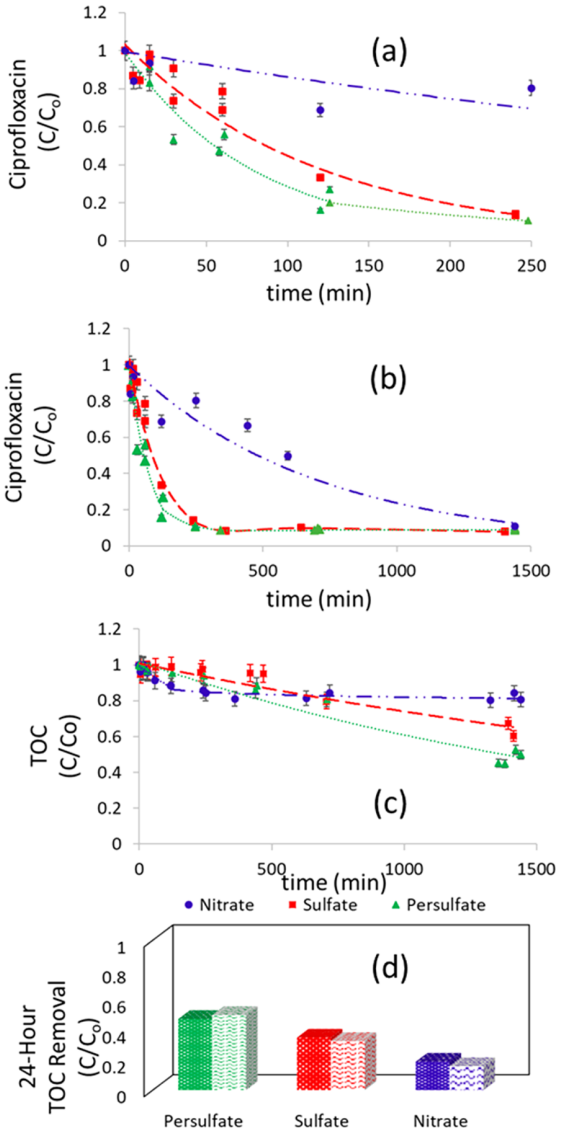

Figure 3. (a) Initial time points for removal of ciprofloxacin versus time; (b) 24 h removal of ciprofloxacin versus time; (c) total organic carbon removal versus time; (d) total organic carbon removal from ciprofloxacin after 24 h. $[Persulfate]_0$ or $[Sulfate]_0$ = 22 mmol L^{-1}. $[Nitrate]_0$ = 66 mmol L^{-1}. $[Ciprofloxacin]_0$ = 0.043 mmol L^{-1}. Experiments completed in a single-cell RDE reactor at 76 mA cm^{-2} anodic current density and 1.33 mA cm^{-2} cathodic current density. BDD anode and Gr cathode.

Comparison of 24 h removal rates is shown in Figure 3d. For both environmentally relevant parameters, ciprofloxacin and TOC removal, EAP offers an advantage for degradation and may be the best approach for some EAOP applications.

Figure S3 shows the specific energy consumption for the data in Figure 3. Energy consumption per unit mass of TOC removed was calculated using eq S3 and presented in Table 1. Energy consumption for persulfate and sulfate electrolytes was in line with that determined for electro-Fenton degradation of enrofloxacin using a BDD anode.[40]

Persulfate was measured during ciprofloxacin reactions in both sulfate and persulfate electrolytes (Figure S4a,b). Ultimately, persulfate reduced to sulfate (Figure S5), with 1.99 mol sulfate formed for every mole persulfate decomposed. In ciprofloxacin−persulfate solutions, persulfate did not follow the same kinetics as in experiments without organic analyte. Persulfate decayed following a pseudo-first-order mechanism with respect to persulfate, with R^2 = 0.99 (Figure S4b). The pseudo-first-order kinetics indicates that, in addition to surface-based persulfate decomposition and generation, there are bulk persulfate reactions that depend on the persulfate concentration, which include possible interactions between persulfate and ciprofloxacin or persulfate and organic radicals. In fact, although both ciprofloxacin decay and persulfate decomposition model well as pseudo-first-order mechanisms with respect to themselves (the typical kinetic model used in environmental remediation studies[21]), there is a second-order relationship between persulfate and ciprofloxacin, shown in Figure S6. The second-order reaction rate constant, calculated by eq S4, is 2.1 × 10^{-2} L mol^{-1} s^{-1} with R^2 = 0.95.[41] In sulfate, persulfate level increased in a nonuniform fashion, likely due to the complex set of reactions including sulfate radicals degrading ciprofloxacin, persulfate activation, and interaction between ciprofloxacin and persulfate.

Radical Roles in Ciprofloxacin Degradation. Quenching studies examined hydroxyl and sulfate radical roles in ciprofloxacin removal. Rate constants for quenchers or ciprofloxacin with radicals are outlined in Table S3. During DMSO quenching, virtually all radicals were predicted to react with DMSO over ciprofloxacin (eq S5a,b).[42] With DMSO addition, only 12% removal was observed in the nitrate solution (Figure S7). Therefore, a portion of the removal in the nitrate solution, under nonquenched conditions, was attributed to hydroxyl radicals, with electrode surface reactions, such as direct oxidation, contributing the remaining portion. In sulfate or persulfate, a substantial reduction in removal was also observed during DMSO quenching. However, in these cases a significant portion of degradation under nonquenched conditions was attributed to both hydroxyl and sulfate radicals. While TBA is typically used to distinguish between sulfate and

Table 1. Effects of Electrolytes on Removal Rates of Ciprofloxacin and TOC[a]

Analyte	Electrolyte	Pseudo-first-order rate constant (s^{-1} × 10^{-4})	Pseudo-first-order fit (R^2)	Rate Constant Difference from Persulfate (%)	Statistical Significance of Difference	Energy Consumption per Unit Mass (kWh (g^{-1}))
Ciprofloxacin	persulfate	2.08 ± 0.58	0.9112			
	sulfate	1.39 ± 0.14	0.9717	33%	>99% (p < 0.0039)	
	nitrate	0.24 ± 0.05	0.9517	88%	>99% (p < 0.0001)	
TOC	persulfate	0.083 ± 0.013	0.9396			0.428
	sulfate	0.043 ± 0.010	0.8582	48%	>99% (p < 0.0001)	0.578
	nitrate	0.0061 ± 0.018	0.317	93%	>99% (p < 0.0001)	1.60

[a]± Denotes 95% confidence intervals.

DOI: 10.1021/acs.est.8b00015
Environ. Sci. Technol. 2018, 52, 5875−5883

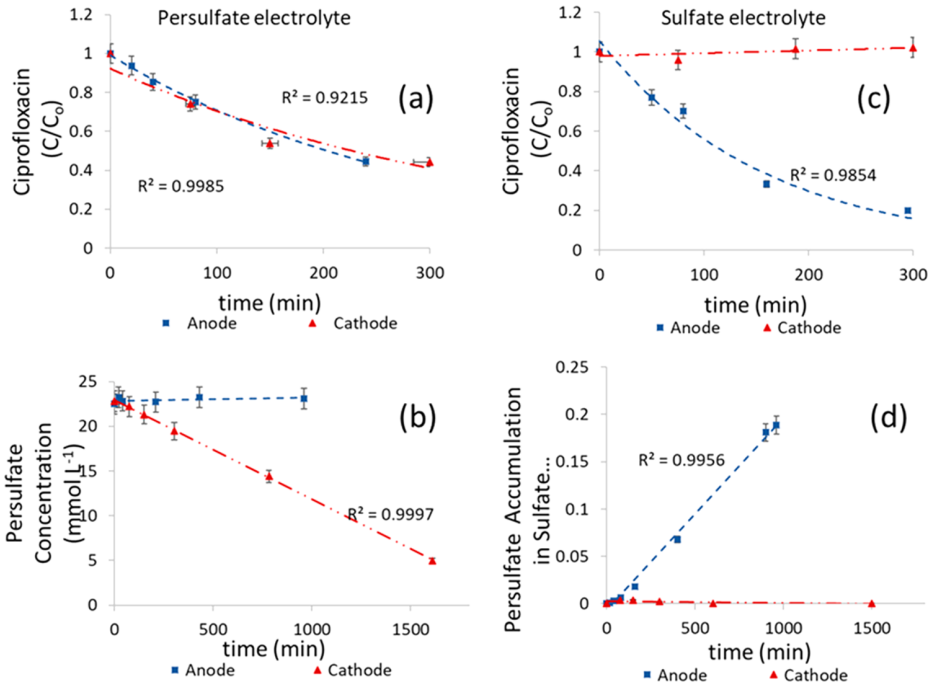

Figure 4. Ciprofloxacin removal and corresponding persulfate concentration in a split-cell RDE. Anodic current density = 28.5 mA cm^{-2}. Cathodic current density = 1.33 mA cm^{-2}. [Ciprofloxacin]$_0$ = 0.043 mmol L^{-1}. (a,b) [Persulfate]$_0$ 22 mmol L^{-1}. (c-d) [Sulfate]$_0$ = 22 mmol L^{-1}.

hydroxyl radicals, calculations (eq S5c,d) did not predict a significant difference in its ability to preferentially quench sulfate radicals over hydroxyl radicals under current experimental conditions. Differences in removal between the two quenchers may be attributable to actual differences in hydroxyl versus sulfate radical reactivity, or may be due to differences in the ability of quenchers to suppress radicals, as established by the competition kinetics fractional calculations (eq S5c,d). Overall, the decreasing ciprofloxacin degradation under quenched conditions suggests that one or both radicals play a significant role in ciprofloxacin degradation using EAP. Of note is the ∼35% removal achieved in persulfate with primary radicals quenched. Radicals such as persulfate ($S_2O_8^{2-}$), R· (organic), and ROO· (organo-peroxide) may propagate from sulfate and hydroxyl radicals but have limited potential to form because their parent radical is quenched.[18,43−45] It is suggested that nonradical based persulfate activation at the BDD anode is partially responsible for enhanced ciprofloxacin removal in persulfate, which has recently been observed in other persulfate-based systems.[11,46,47]

Cyclic Voltammetry. Cyclic voltammograms (C-Vs) were created/measured to clarify differences between electrolytes for persulfate activation and ciprofloxacin abatement. Two distinct oxidation peaks for ciprofloxacin were observed at the BDD anode (Figure S8) in all electrolytes, demonstrating that surface-based oxidation of ciprofloxacin is likely partially responsible for the ciprofloxacin removal shown in Figure 3. A third oxidation peak was marginally visible in sulfate and nitrate, but was more prominent in persulfate, revealing that persulfate electrolyte may drive oxidation at a lower voltage. Full C-Vs are shown in Figure S9. Multicycle C-Vs (Figure S10), demonstrate ciprofloxacin oxidation is a quasi-irreversible process, as there are no symmetric reduction peaks and the oxidation peaks almost disappear after the first cycle. Scan rates of 100 mV s^{-1} established the limiting current, from which the mass-transfer coefficient in each electrolyte was calculated using eq S6 as outlined by Cañizares et al. (2006).[48] The mass-coefficient more than doubles going from nitrate to sulfate electrolyte, and increases an additional 35% in persulfate. Better transfer of the analyte to the electrode surface may play a part in the increased reactivity of ciprofloxacin in persulfate. In Figure S11a, the peak current at the anode (ln $I_{p,a}$) versus the square root of scan rate ($v^{1/2}$) is illustrated for peaks 1 and 2 from Figure S8. The linear relationships (all $r^2 > 0.93$) indicate diffusion controlled processes.[49] Figure S11b shows the linear relationship between anodic voltage ($E_{we,a}$) at the peak current and ln v. Based on the diffusion process established in Figure S11a, eq S7 was used to calculate values of the charge transfer coefficient × number electrons (αn) involved in the electrochemical process.[49] These values are listed in Table S5, with $\alpha n = \alpha$ when $n = 1$.

C-Vs were also completed for graphite and platinum material (Figure S12), with focus on the reductive reactions occurring at these cathodes (Figure S13). For nitrate and sulfate electrolytes, there were no significant differences between cathode materials. Direct reduction of ciprofloxacin was not observed in the potential range evaluated. An irreversible reduction peak at both cathodes is observed when persulfate and ciprofloxacin are present in solution together. This indicates a surface-based reaction between persulfate and ciprofloxacin, i.e., direct electrochemical persulfate activation. For the platinum/persulfate curve, the reduction peak and corresponding sharp oxidation peak at a similar negative potential is indicative of an adsorption/desorption process for ciprofloxacin, which is often seen with organic analytes on platinum or gold electrodes.[50,51] The mass transfer coefficients calculated for persulfate−ciprofloxacin peaks in Figure S12 are not statistically different at 2.02 × 10^{-4} m s^{-1} for Gr and 1.90 × 10^{-4} m s^{-1} for Pt (eq S6, assuming $n = 1$), matching degradation results that concluded these electrodes have similar efficacy for EAP.

DOI: 10.1021/acs.est.8b00015
Environ. Sci. Technol. 2018, 52, 5875−5883

Using Ciprofloxacin To Evaluate Persulfate Activation. Further verification of electrochemical persulfate activation was established with ciprofloxacin electrolysis in a split-cell RDE with BDD/Gr electrodes. Figure 4 shows a well-defined difference in ciprofloxacin removal at the cathode in persulfate with pseudo-first-order (R^2 = 0.9215) degradation with respect to ciprofloxacin in persulfate and 55% removal within 300 min (Figure 4a) versus no removal in sulfate electrolyte (Figure 4c). These results, combined with C−V analysis, provide strong experimental evidence of persulfate activation at the cathode, verifying what other studies have previously postulated.[23,24] While persulfate transformation at the anode did not occur (Figure 4b) and sulfate was not available to form sulfate radicals, some ciprofloxacin removal was still observed at the anode in persulfate, with reaction rates of 1.1×10^{-4} s^{-1} and 5.1×10^{-5} s^{-1} in sulfate and persulfate, respectively. Quenching results suggested nonradical persulfate activation at the BDD anode may account for ciprofloxacin removal in the anode cell.

Persulfate activation and regeneration were observed with organic analyte in solution (Figure 4b,d) as without organic analyte (Figure 1b,c). Persulfate decomposition at the cathode (Figure 4b) did not exhibit pseudo-first-order decay with respect to persulfate, as seen in the single-cell solution even though ciprofloxacin was present. This pseudo-first-order mechanism may result from a synergistic effect between reactions at the anode and cathode.

Ciprofloxacin Transformation. Ciprofloxacin transformation pathways were examined for the three electrolytes, as shown in Figure S14. Mass spectra corresponding to byproducts shown in Figure S14 are presented in Figure S16a−u. In persulfate, rapid defluorination occurred within 15 min (Figure S15), corresponding to the rapid ciprofloxacin removal observed in Figure 3a. Figure S17a−g shows the ciprofloxacin transformation through hydroxyl radical attack for different mechanisms that can take place. A multipoint hydroxylation with fluoride substitution (Figure S14), through m/z 362, was identified as a dominant route for ciprofloxacin breakdown in persulfate. Figure S17a further illustrates the multipoint hydroxylation with formation of m/z 348, 346, and 362 and further hydroxyl radical substitution of the piperazine ring producing m/z 294. Similar mechanisms involving hydroxylation and/or defluorination were observed in multiple studies using either electrochemical oxidation or activated-persulfate degradation.[13,26,45,52,53] As hydroxyl radical production occurs during both degradation processes, this further suggests that hydroxyl radicals played a role in the ciprofloxacin breakdown. Ciprofloxacin defluorination reached >90% in both persulfate and sulfate, which is important because defluorination may lower toxic effects of fluorinated contaminants.[53] Defluorination in nitrate only reached 36%, which was much slower than in the sulfate and persulfate solutions. Fluoride removal in sulfate and nitrate was almost linear, indicating a surface-dominated mechanism, whereas the persulfate solution increased exponentially signifying defluorination dependence on hydroxyl radical concentration.

Hydroxylation without defluorination observed through the production of m/z 264 was a major degradation route in all electrolytes and the dominant pathway in nitrate and sulfate. This suggests that hydroxyl radical production was a major contributor to ciprofloxacin degradation in these solutions. Two pathways that could take place are shown in Figure S17b,c. In both routes, hydroxylation and substitution of the piperazine ring eventually lead to the formation of m/z 296.

A third pathway, breakdown of the core quinolone structure through m/z 328 production, was shown in all electrolytes (Figure S14) and was comparable to results observed in other studies.[13,45] This again suggests hydroxyl radical production plays a major role in ciprofloxacin degradation. Additional key mechanisms observed in this and other ciprofloxacin degradation studies include: (1) piperazine-ring cleavage with the detection of m/z 362, 294, 274, and 264 (Figure S17d),[13,26,45,52−54] (2) cyclo-propyl group breakdown with the formation of m/z 270, 240, and 234 (Figure S17e),[13] (3) loss of amines with the formation of m/z 270, 294, and 264 (Figure S17f),[13,52] and (4) decarboxylation with the formation of m/z of 270 and 254 (Figure S17g).[45,52,54] These reactions indicate that different sites on the ciprofloxacin molecule are attacked through different mechanisms. Though significant differences were seen based on the electrolytes, no significant differences were noted between cathode materials. While no sulfate-adducts were observed, possible nitrate-adduct formation indicates potential nitrate radical evolution at the BDD anode in nitrate. Overall, electrochemically generated sulfate radicals resulted in additional degradation pathways corresponding to the enhanced ciprofloxacin and TOC removal observed in sulfate and persulfate solutions.

Based on this study's results, anodic sulfate radical formation, anodic nonradical persulfate activation and cathodic persulfate activation are expected to contribute to accelerated removal rates of organic analytes susceptible to activated persulfate reactions. This study screened EAP as a viable candidate for point source treatment of wastewaters contaminated by fluoroquinilone antibiotics like ciprofloxacin. Future work should include analysis of reactions in real-water matrices (including presence of inorganic ions and high TOC levels) and application to other analytes. Reactor design must also be considered, including flow-through single-cell reactors, where mass transfer limitations to electrode surface might impact the system's ability to effectively activate persulfate and subsequently degrade antibiotics. Further investigation is warranted in determining the efficacy of EAP for real-world application.

■ ASSOCIATED CONTENT

Supporting Information

The Supporting Information is available free of charge on the ACS Publications website at DOI: 10.1021/acs.est.8b00015.

Single-cell reactor with rotating disk electrode (RDE) (Schematic S1b); split-cell reactor with rotating disk electrode (RDE) (Method S1); LC-MS method for ciprofloxacin byproduct detection (eq S1); normalization of reaction time based on reactor volumes (eq S2); electrochemical hydrogen peroxide evolution (eq S3); energy consumption per unit mass TOC (eq S4); second-order kinetic model (eq S5a−d); competition kinetics for ciprofloxacin in quenchers (eq S6); mass-transfer coefficient (Table S1); HPLC multistep gradient program (Table S2a); effects of cathodes on removal rates of ciprofloxacin (Table S2b); effects of cathodes on removal rates of TOC (Table S3); reaction rate constants of quenching experiments (Table S4); mass-transfer coefficients of ciprofloxacin in electrolytes (Table S5); charge transfer coefficient, α Figure S1; pseudo-first-

DOI: 10.1021/acs.est.8b00015
Environ. Sci. Technol. 2018, 52, 5875−5883

order kinetics for degradation of ciprofloxacin (Figure S2); initial stages of ciprofloxacin degradation (Figure S3); ciprofloxacin removal versus specific electrical charge (Figure S4); persulfate behavior during ciprofloxacin degradation (Figure S5); persulfate reduction to sulfate (Figure S6); second-order reaction modeling of ciprofloxacin and persulfate (Figure S7); quenching experiments (Figure S8); ciprofloxacin oxidation peak during cyclic voltammetry using a BDD anode (Figure S9); complete cyclic voltammetry of ciprofloxacin in nitrate, sulfate or persulfate using a BDD anode at different scan rates (Figure S10); multiple-cycle cyclic voltammetry of ciprofloxacin in nitrate, sulfate or persulfate using a BDD anode (Figure S11); modeling of C-V scans for Ciprofloxacin (Figure S12); complete cyclic voltammetry of ciprofloxacin in nitrate, sulfate and persulfate using Pt or Gr (Figure S13); reduction peak during cyclic voltammetry of cathode materials (Figure S14); ciprofloxacin transformation pathways (Figure S15); defluorination of 0.043 mmol L^{-1} ciprofloxacin with a BDD anode and graphite or platinum cathode (Figure S16); mass spectra for byproducts are shown for (a–h) nitrate, (i) sulfate, and (j–u) persulfate at various time points during the degradation of ciprofloxacin (Figure S17); ciprofloxacin transformation through hydroxyl radical attack for (a) multipoint hydroxylation, piperazine substitution and defluorination, (b) hydroxylation without defluorination, (c) hydroxylation without defluorination, (d) piperazaine-ring cleavage, (e) cyclopropyl group breakdown, (f) amine loss, and (g) decarboxylation (PDF)

AUTHOR INFORMATION

Corresponding Author

*Kimberly E. Carter, Phone: (865) 974-7731; Email: kcarte46@utk.edu.

ORCID

Kimberly E. Carter: 0000-0002-8114-1248

Notes

The authors declare no competing financial interest.

ACKNOWLEDGMENTS

The authors thank Dr. John S. Schwartz and Adrian Gonzalez for assistance with ion chromatography, and Dr. Hector Castro and Dr. Shawn Campagna (Biological and Small Molecule Mass Spectrometry Core, University of Tennessee) for assistance with HPLC-MS.

REFERENCES

(1) Yuan, X. J.; Qiang, Z. M.; Ben, W. W.; Zhu, B.; Qu, J. H. Distribution, mass load and environmental impact of multiple-class pharmaceuticals in conventional and upgraded municipal wastewater treatment plants in East China. *Environ. Sci-Proc. Imp* **2015**, *17* (3), 596–605.

(2) Ory, J.; Bricheux, G.; Togola, A.; Bonnet, J. L.; Donnadieu-Bernard, F.; Nakusi, L.; Forestier, C.; Traore, O. Ciprofloxacin residue and antibiotic-resistant biofilm bacteria in hospital effluent. *Environ. Pollut.* **2016**, *214*, 635–645.

(3) Papageorgiou, M.; Kosma, C.; Lambropoulou, D. Seasonal occurrence, removal, mass loading and environmental risk assessment of 55 pharmaceuticals and personal care products in a municipal wastewater treatment plant in Central Greece. *Sci. Total Environ.* **2016**, *543*, 547–569.

(4) Helwig, K.; Hunter, C.; McNaughtan, M.; Roberts, J.; Pahl, O. Ranking Prescribed Pharmaceuticals in Terms of Environmental Risk: Inclusion of Hospital Data and the Importance of Regular Review. *Environ. Toxicol. Chem.* **2016**, *35* (4), 1043–1050.

(5) Ji, K.; Han, E. J.; Back, S.; Park, J.; Ryu, J.; Choi, K. Prioritizing Human Pharmaceuticals for Ecological Risks in the Freshwater Environment of Korea. *Environ. Toxicol. Chem.* **2016**, *35* (4), 1028–1036.

(6) Mutiyar, P. K.; Mittal, A. K. Risk assessment of antibiotic residues in different water matrices in India: key issues and challenges. *Environ. Sci. Pollut. Res.* **2014**, *21* (12), 7723–7736.

(7) Santos, L. H. M. L. M.; Gros, M.; Rodriguez-Mozaz, S.; Delerue-Matos, C.; Pena, A.; Barceló, D.; Montenegro, M. C. B. S. M. Contribution of hospital effluents to the load of pharmaceuticals in urban wastewaters: Identification of ecologically relevant pharmaceuticals. *Sci. Total Environ.* **2013**, *461–462*, 302–316.

(8) Du, L. F.; Liu, W. K. Occurrence, fate, and ecotoxicity of antibiotics in agro-ecosystems. A review. *Agron. Sustainable Dev.* **2012**, *32* (2), 309–327.

(9) Mackul'ak, T.; Vojs, M.; Grabic, R.; Golovko, O.; Stanova, A. V.; Birosova, L.; Medved'ova, A.; Hives, J.; Gal, M.; Kromka, A.; Hanusova, A. Occurrence of pharmaceuticals, illicit drugs, and resistant types of bacteria in hospital effluent and their effective degradation by boron-doped diamond electrodes. *Monatsh. Chem.* **2016**, *147* (1), 97–103.

(10) Jara, C. C.; Fino, D.; Specchia, V.; Saracco, G.; Spinelli, R. Electrochemical removal of antibiotics from wastewaters. *Appl. Catal., B* **2007**, *70* (1–4), 479–487.

(11) Farhat, A.; Keller, J.; Tait, S.; Radjenovic, J. Removal of Persistent Organic Contaminants by Electrochemically Activated Sulfate. *Environ. Sci. Technol.* **2015**, *49* (24), 14326–14333.

(12) Miyata, M.; Ihara, I.; Yoshid, G.; Toyod, K.; Umetsu, K. Electrochemical oxidation of tetracycline antibiotics using a Ti/IrO_2 anode for wastewater treatment of animal husbandry. *Water Sci. Technol.* **2011**, *63* (3), 456–461.

(13) Antonin, V. S.; Santos, M. C.; Garcia-Segura, S.; Brillas, E. Electrochemical incineration of the antibiotic ciprofloxacin in sulfate medium and synthetic urine matrix. *Water Res.* **2015**, *83*, 31–41.

(14) Sirés, I.; Brillas, E. Remediation of water pollution caused by pharmaceutical residues based on electrochemical separation and degradation technologies: A review. *Environ. Int.* **2012**, *40*, 212–229.

(15) Radjenovic, J.; Sedlak, D. L. Challenges and Opportunities for Electrochemical Processes as Next-Generation Technologies for the Treatment of Contaminated Water. *Environ. Sci. Technol.* **2015**, *49* (19), 11292–11302.

(16) Garcia-Segura, S.; Keller, J.; Brillas, E.; Radjenovic, J. Removal of organic contaminants from secondary effluent by anodic oxidation with a boron-doped diamond anode as tertiary treatment. *J. Hazard. Mater.* **2015**, *283*, 551–557.

(17) Weiss, E.; Groenen-Serrano, K.; Savall, A. Electrochemical mineralization of sodium dodecylbenzenesulfonate at boron doped diamond anodes. *J. Appl. Electrochem.* **2007**, *37* (11), 1337–1344.

(18) Sirés, I.; Brillas, E.; Oturan, M. A.; Rodrigo, M. A.; Panizza, M. Electrochemical advanced oxidation processes: today and tomorrow. A review. *Environ. Sci. Pollut. Res.* **2014**, *21* (14), 8336–8367.

(19) Carter, K. E.; Farrell, J. Electrochemical Oxidation of Trichloroethylene Using Boron-Doped Diamond Film Electrodes. *Environ. Sci. Technol.* **2009**, *43* (21), 8350–8354.

(20) Radjenovic, J.; Petrovic, M. Sulfate-mediated electrooxidation of X-ray contrast media on boron doped diamond anode. *Water Res.* **2016**, *94*, 128–135.

(21) Matzek, L. W.; Carter, K. E. Activated persulfate for organic chemical degradation: A review. *Chemosphere* **2016**, *151*, 178–188.

(22) Matzek, L. W.; Carter, K. E. Sustained persulfate activation using solid iron: Kinetics and application to ciprofloxacin degradation. *Chem. Eng. J.* **2017**, *307*, 650–660.

(23) Chen, W. S.; Jhou, Y. C.; Huang, C. P. Mineralization of dinitrotoluenes in industrial wastewater by electro-activated persulfate oxidation. *Chem. Eng. J.* **2014**, *252*, 166–172.

DOI: 10.1021/acs.est.8b00015
Environ. Sci. Technol. 2018, 52, 5875–5883

(24) Chen, W.-S.; Huang, C.-P. Mineralization of aniline in aqueous solution by electrochemical activation of persulfate. *Chemosphere* **2015**, *125*, 175−181.
(25) Pillai, I. M. S.; Gupta, A. K. Effect of inorganic anions and oxidizing agents on electrochemical oxidation of methyl orange, malachite green and 2,4-dinitrophenol. *J. Electroanal. Chem.* **2016**, *762*, 66−72.
(26) Wang, Y.; Shen, C. C.; Zhang, M. M.; Zhang, B. T.; Yu, Y. G. The electrochemical degradation of ciprofloxacin using a SnO2-Sb/Ti anode: Influencing factors, reaction pathways and energy demand. *Chem. Eng. J.* **2016**, *296*, 79−89.
(27) Menegazzo, N.; Jin, C. M.; Narayan, R. J.; Mizaikoff, B. Compositional and electrochemical characterization of noble metal-diamondlike carbon nanocomposite thin films. *Langmuir* **2007**, *23* (12), 6812−6818.
(28) Tan, C. Q.; Gao, N. Y.; Zhou, S. Q.; Xiao, Y. L.; Zhuang, Z. Z. Kinetic study of acetaminophen degradation by UV-based advanced oxidation processes. *Chem. Eng. J.* **2014**, *253*, 229−236.
(29) Lin, C. C.; Wu, M. S. Degradation of ciprofloxacin by UV/S2O82- process in a large photoreactor. *J. Photochem. Photobiol., A* **2014**, *285*, 1−6.
(30) Liang, C. J.; Bruell, C. J.; Marley, M. C.; Sperry, K. L. Persulfate oxidation for in situ remediation of TCE. II. Activated by chelated ferrous ion. *Chemosphere* **2004**, *55* (9), 1225−1233.
(31) Yuan, S. H.; Liao, P.; Alshawabkeh, A. N. Electrolytic Manipulation of Persulfate Reactivity by Iron Electrodes for Trichloroethylene Degradation in Groundwater. *Environ. Sci. Technol.* **2014**, *48* (1), 656−663.
(32) Oncu, N. B.; Mercan, N.; Balcioglu, I. A. The impact of ferrous iron/heat-activated persulfate treatment on waste sewage sludge constituents and sorbed antimicrobial micropollutants. *Chem. Eng. J.* **2015**, *259*, 972−980.
(33) Cañizares, P.; Sáez, C.; Sánchez-Carretero, A.; Rodrigo, M. Synthesis of novel oxidants by electrochemical technology. *J. Appl. Electrochem.* **2009**, *39* (11), 2143−2149.
(34) Guinea, E.; Centellas, F.; Brillas, E.; Cañizares, P.; Sáez, C.; Rodrigo, M. A. Electrocatalytic properties of diamond in the oxidation of a persistant pollutant. *Appl. Catal., B* **2009**, *89* (3), 645−650.
(35) Liang, C. J.; Huang, C. F.; Mohanty, N.; Kurakalva, R. M. A rapid spectrophotometric determination of persulfate anion in ISCO. *Chemosphere* **2008**, *73* (9), 1540−1543.
(36) Kolthoff, I. M.; Carr, E. M. Volumetric Determination of Persulfate in the Presence of Organic Substances. *Anal. Chem.* **1953**, *25* (2), 298−301.
(37) Nogueira, R. F. P.; Oliveira, M. C.; Paterlini, W. C. Simple and fast spectrophotometric determination of H2O2 in photo-Fenton reactions using metavanadate. *Talanta* **2005**, *66* (1), 86−91.
(38) Davis, J.; Baygents, J. C.; Farrell, J. Understanding Persulfate Production at Boron Doped Diamond Film Anodes. *Electrochim. Acta* **2014**, *150*, 68−74.
(39) Figueroa, S.; Vazquez, L.; Alvarez-Gallegos, A. Decolorizing textile wastewater with Fenton's reagent electrogenerated with a solar photovoltaic cell. *Water Res.* **2009**, *43* (2), 283−294.
(40) Guinea, E.; Garrido, J. A.; Rodriguez, R. M.; Cabot, P. L.; Arias, C.; Centellas, F.; Brillas, E. Degradation of the fluoroquinolone enrofloxacin by electrochemical advanced oxidation processes based on hydrogen peroxide electrogeneration. *Electrochim. Acta* **2010**, *55* (6), 2101−2115.
(41) Clark, M. M. *Transport modeling for environmental engineers and scientists*; John Wiley & Sons, 2011.
(42) von Gunten, U. Ozonation of drinking water: Part I. Oxidation kinetics and product formation. *Water Res.* **2003**, *37* (7), 1443−1467.
(43) Petri, B. G.; Watts, R. J.; Tsitonaki, A.; Crimi, M.; Thomson, N. R.; Teel, A. L. Fundamentals of Isco Using Persulfate. *Serdp Estcp Remediat* **2011**, *3*, 147−191.
(44) Yu, X. Y.; Bao, Z. C.; Barker, J. R. Free radical reactions involving Cl-center dot, Cl-2(-center dot), and SO4-center dot in the 248 nm photolysis of aqueous solutions containing S2O82- and Cl-. *J. Phys. Chem. A* **2004**, *108* (2), 295−308.
(45) Ji, Y. F.; Ferronato, C.; Salvador, A.; Yang, X.; Chovelon, J. M. Degradation of ciprofloxacin and sulfamethoxazole by ferrous-activated persulfate: Implications for remediation of groundwater contaminated by antibiotics. *Sci. Total Environ.* **2014**, *472*, 800−808.
(46) Zhang, T.; Chen, Y.; Wang, Y. R.; Le Roux, J.; Yang, Y.; Croue, J. P. Efficient Peroxydisulfate Activation Process Not Relying on Sulfate Radical Generation for Water Pollutant Degradation. *Environ. Sci. Technol.* **2014**, *48* (10), 5868−5875.
(47) Lee, H.; Lee, H.-J.; Jeong, J.; Lee, J.; Park, N.-B.; Lee, C. Activation of persulfates by carbon nanotubes: Oxidation of organic compounds by nonradical mechanism. *Chem. Eng. J.* **2015**, *266*, 28−33.
(48) Cañizares, P.; García-Gómez, J.; Fernández de Marcos, I.; Rodrigo, M. A.; Lobato, J. Measurement of Mass-Transfer Coefficients by an Electrochemical Technique. *J. Chem. Educ.* **2006**, *83* (8), 1204.
(49) Guidelli, R.; Compton, R. G.; Feliu, J. M.; Gileadi, E.; Lipkowski, J.; Schmickler, W.; Trasatti, S. Definition of the transfer coefficient in electrochemistry (IUPAC Recommendations 2014). *Pure Appl. Chem.* **2014**, *86*, 259−262.
(50) Förster, R. J.; O'Kelly, J. P. Dynamics of [Os(bpy) 2 (p3p) 2] 2+ adsorption and desorption on platinum and gold microelectrodes. *J. Electrochem. Soc.* **2001**, *148* (1), E31−E37.
(51) Masuda, T.; Ikeda, K.; Uosaki, K. Potential-Dependent Adsorption/Desorption Behavior of Perfluorosulfonated Ionomer on a Gold Electrode Surface Studied by Cyclic Voltammetry, Electrochemical Quartz Microbalance, and Electrochemical Atomic Force Microscopy. *Langmuir* **2013**, *29* (7), 2420−2426.
(52) Yahya, M. S.; Oturan, N.; El Kacemi, K.; El Karbane, M.; Aravindakumar, C. T.; Oturan, M. A. Oxidative degradation study on antimicrobial agent ciprofloxacin by electro-fenton process: Kinetics and oxidation products. *Chemosphere* **2014**, *117*, 447−454.
(53) Perini, J. A. D.; Silva, B. F.; Nogueira, R. F. P. Zero-valent iron mediated degradation of ciprofloxacin - Assessment of adsorption, operational parameters and degradation products. *Chemosphere* **2014**, *117*, 345−352.
(54) Guo, H. G.; Gao, N. Y.; Yang, Y.; Zhang, Y. L. Kinetics and transformation pathways on oxidation of fluoroquinolones with thermally activated persulfate. *Chem. Eng. J.* **2016**, *292*, 82−91.

DOI: 10.1021/acs.est.8b00015
Environ. Sci. Technol. 2018, 52, 5875−5883